*In all structural representations, enterobactin is shown in green, Fe ions as red spheres, and interacting residues in yellow. LIGPLOT+ diagrams represent hydrogen bonds as green dashed lines and hydrophobic interactions as red arcs.

** Note: Fe(III) is not explicitly represented in LIGPLOT+ diagrams, as the software does not depict metal ions; interactions shown correspond to enterobactin–protein contacts.

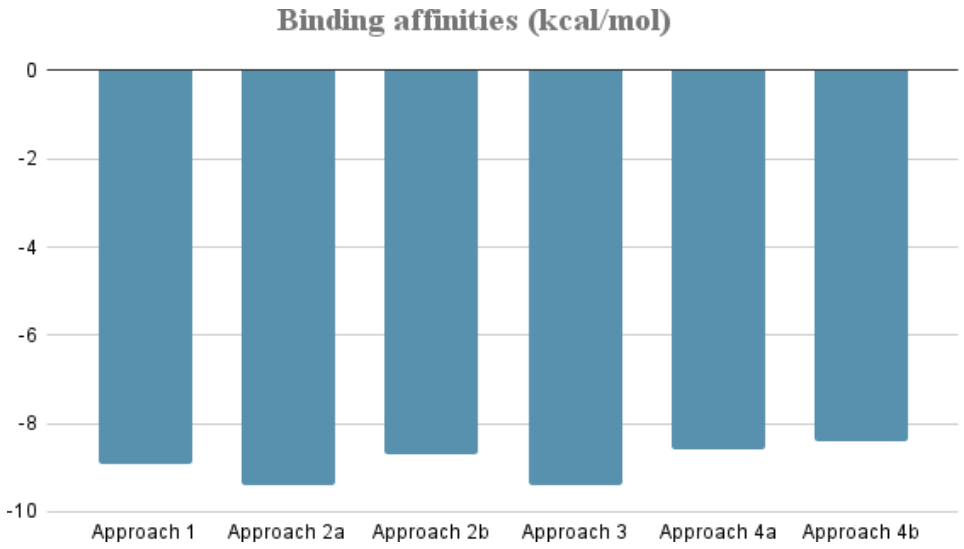


Figure S1: Most negative binding affinities (kcal/mol) obtained from the docking approaches outlined in Table 1.

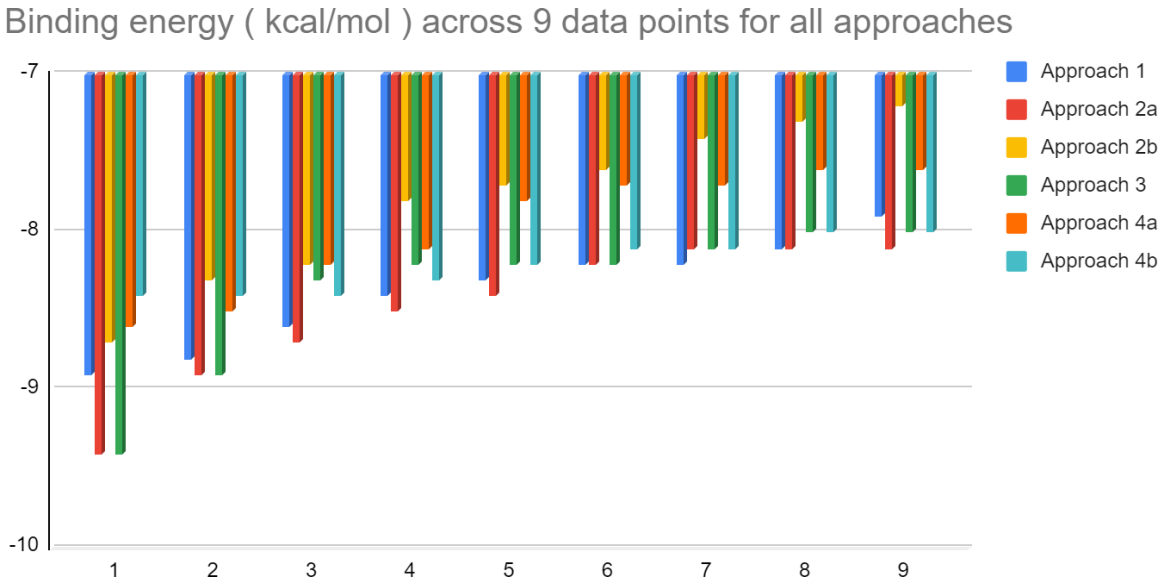
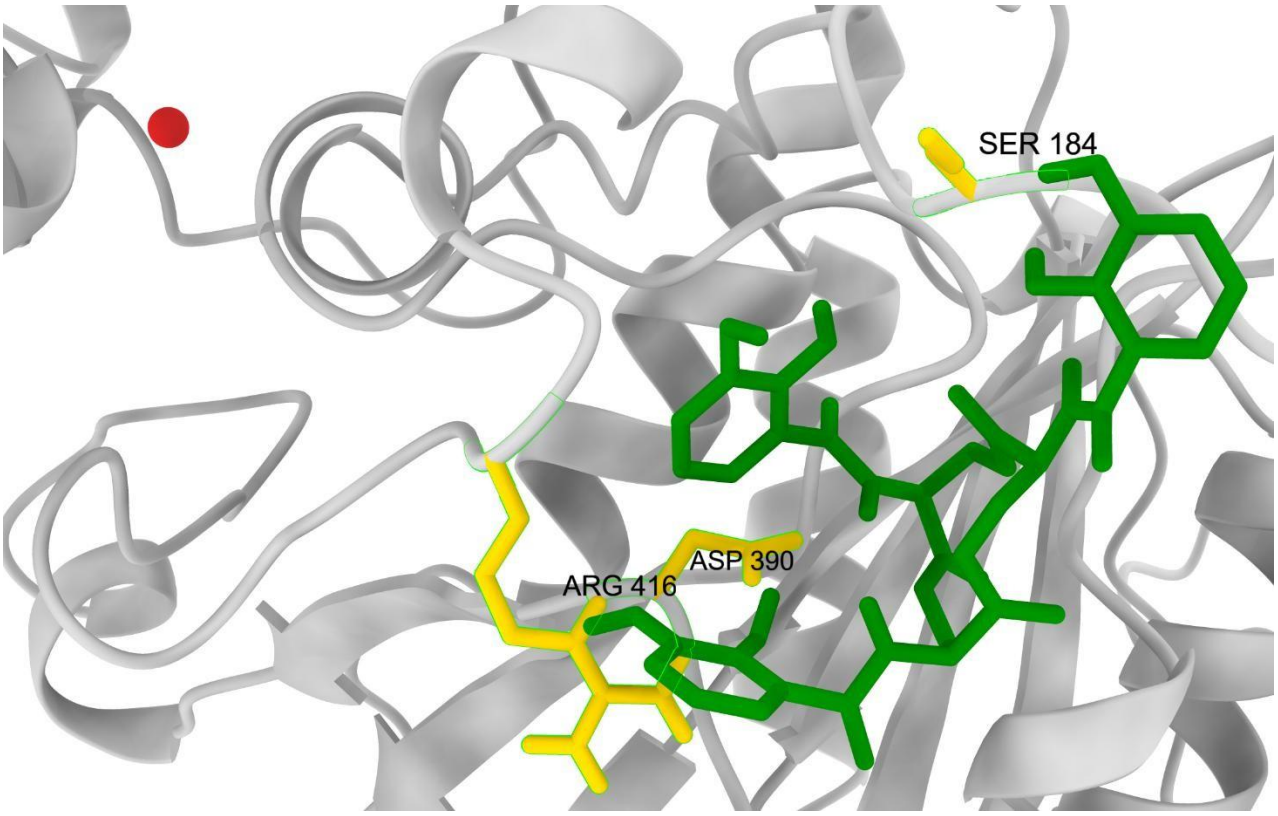


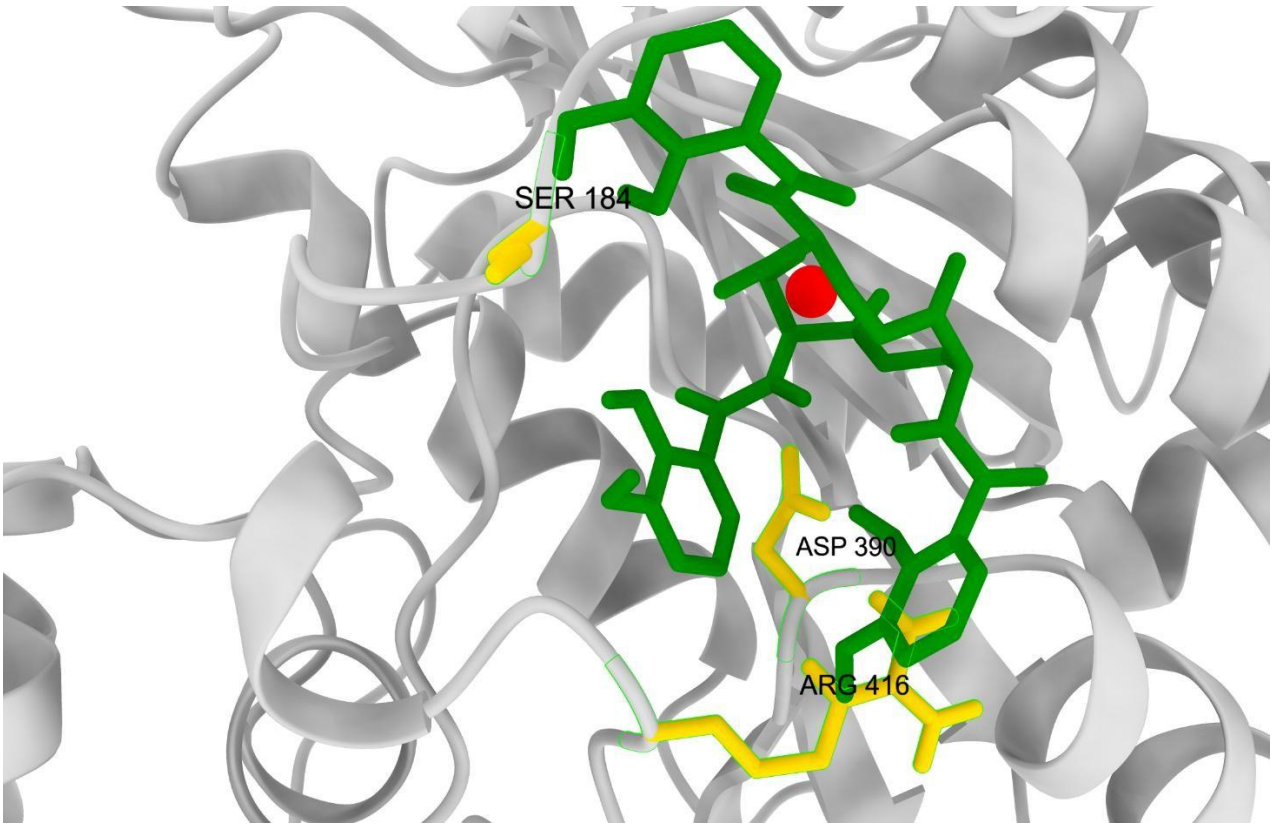
Figure S2: Binding affinities (kcal/mol) across nine docking conformations for each approach (Table 1).

The most stable conformations (labelled 1) show the lowest binding energies for approaches 2a and 3.

A



B



C

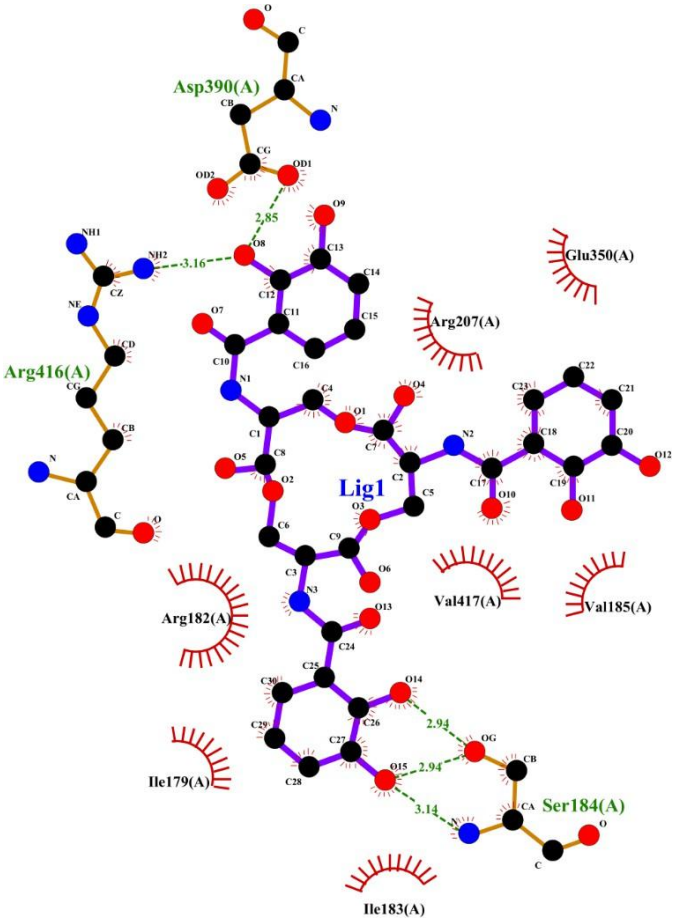


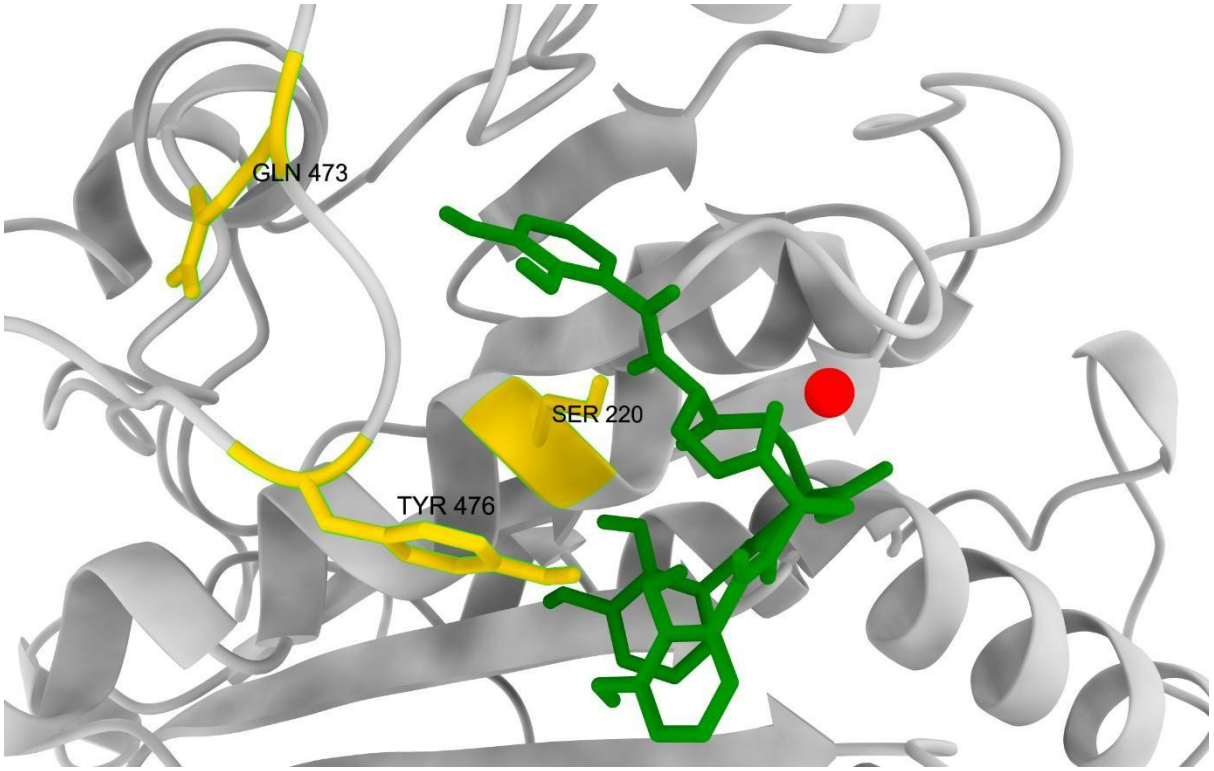
Figure S3: Approach 1.

(A) Docking snapshot showing the most stable conformation. Enterobactin is shown in green, Fe(III) as a red sphere, and interacting residues in yellow (Arg416, Ser184, Asp390).

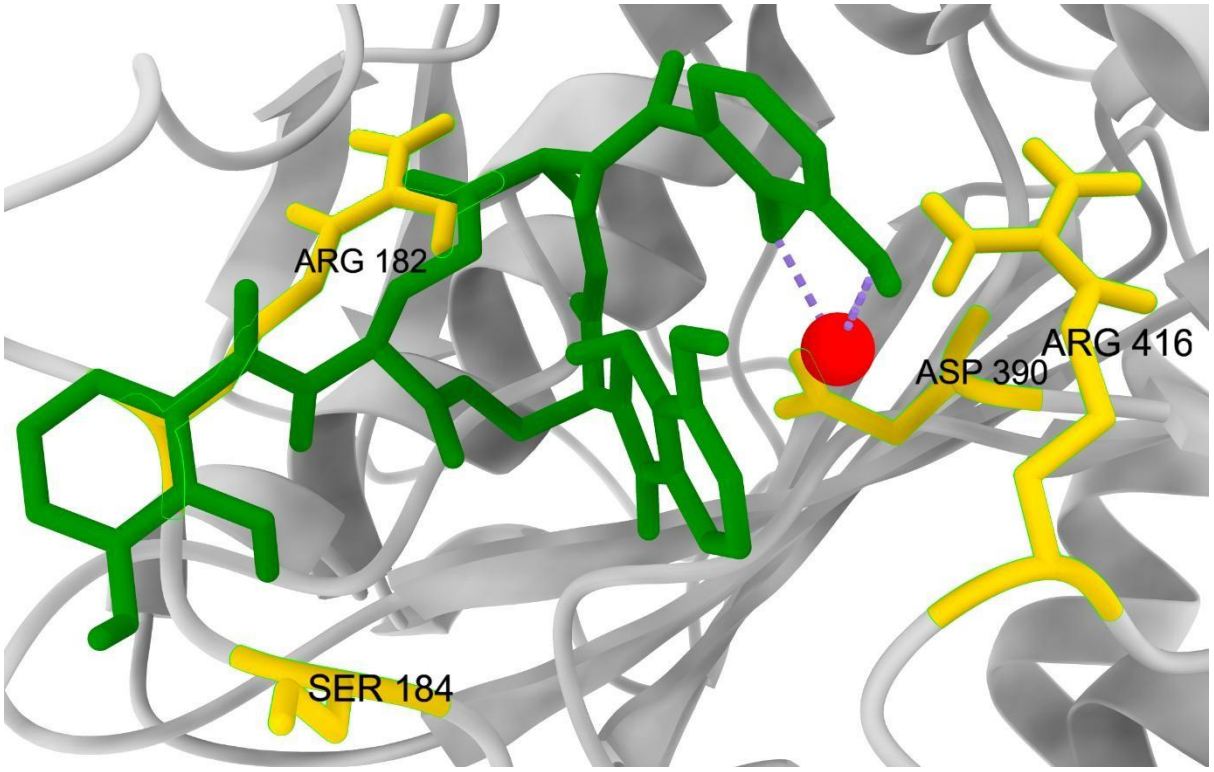
(B) Docking snapshot of the second most stable conformation.

(C) Corresponding LIGPLOT+ interaction diagram. Hydrogen bonds are shown as green dashed lines and hydrophobic interactions as red arcs.

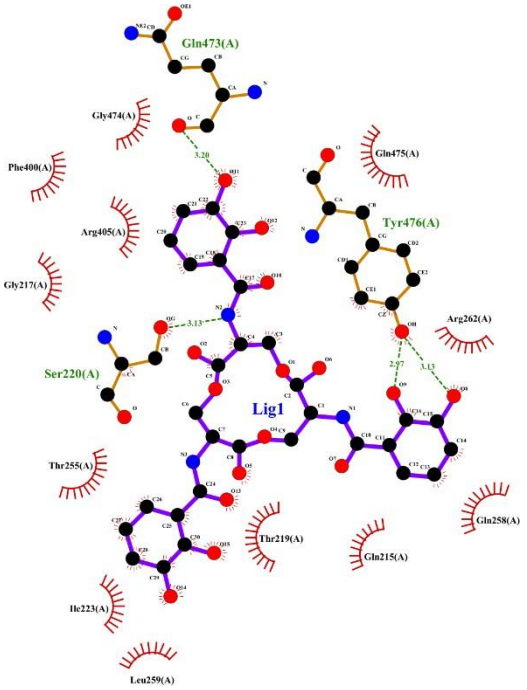
A



B



C



D

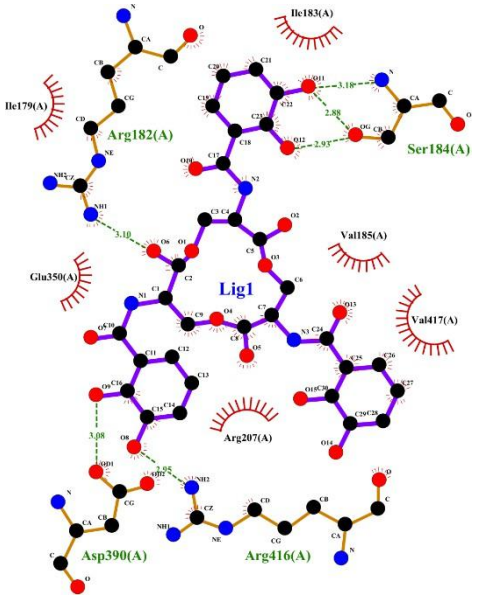


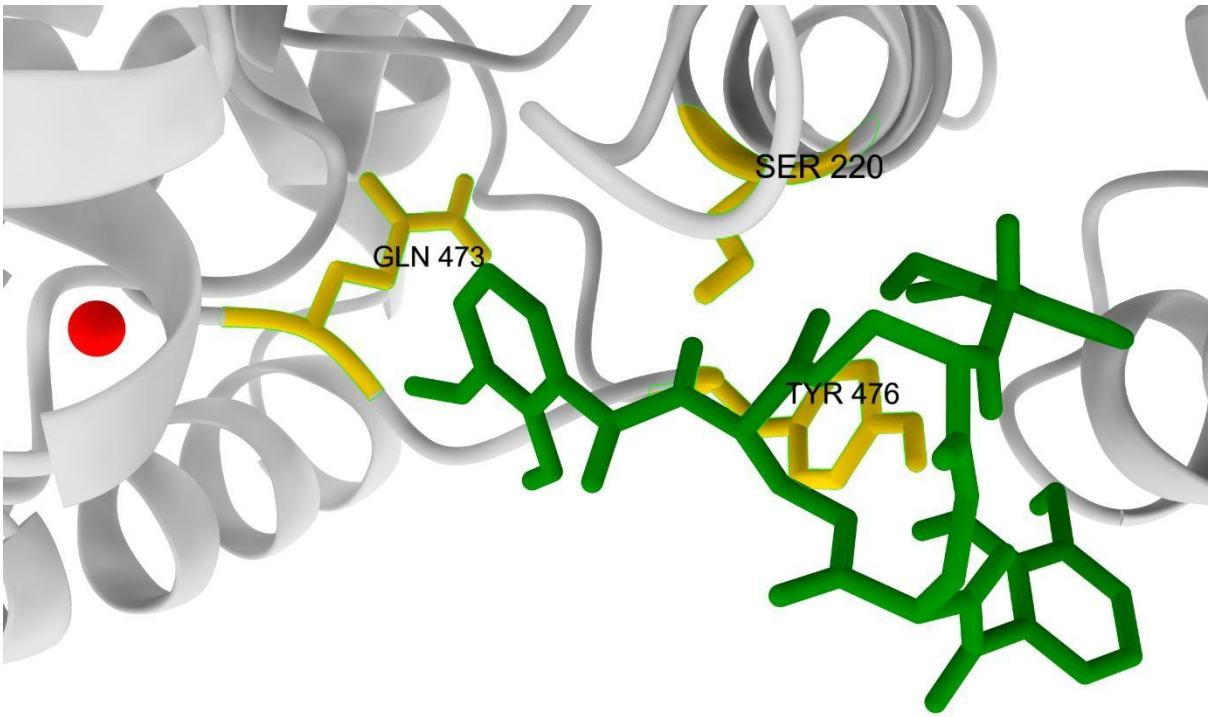
Figure S4: Approach 2.

(A) Most stable conformation obtained after docking for Approach 2a. Interacting residues (Ser220, Gln473, Tyr476) are shown in yellow.

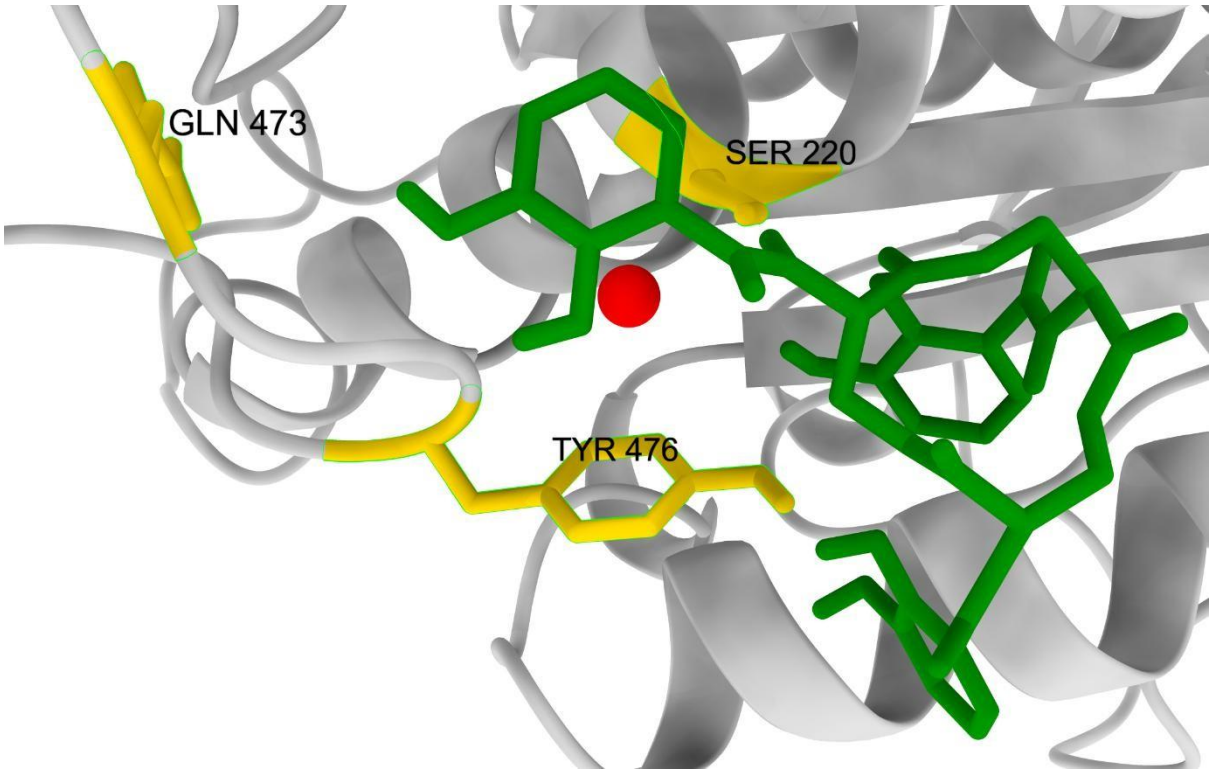
(B) Most stable conformation obtained after docking for Approach 2b. Interacting residues (Arg182, Ser184, Asp390, Arg416) are shown in yellow.

(C–D) Corresponding LIGPLOT+ interaction diagrams for Approaches 2a and 2b, respectively.

A



B



C

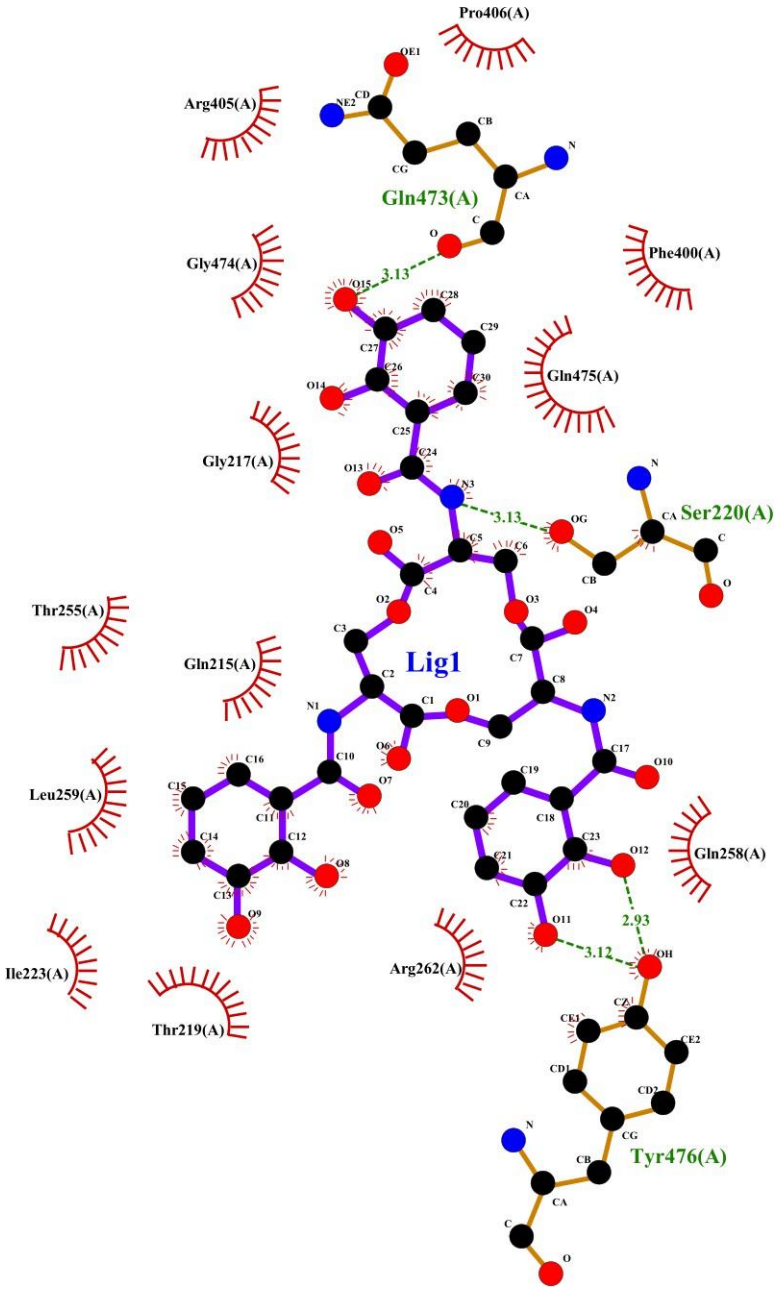


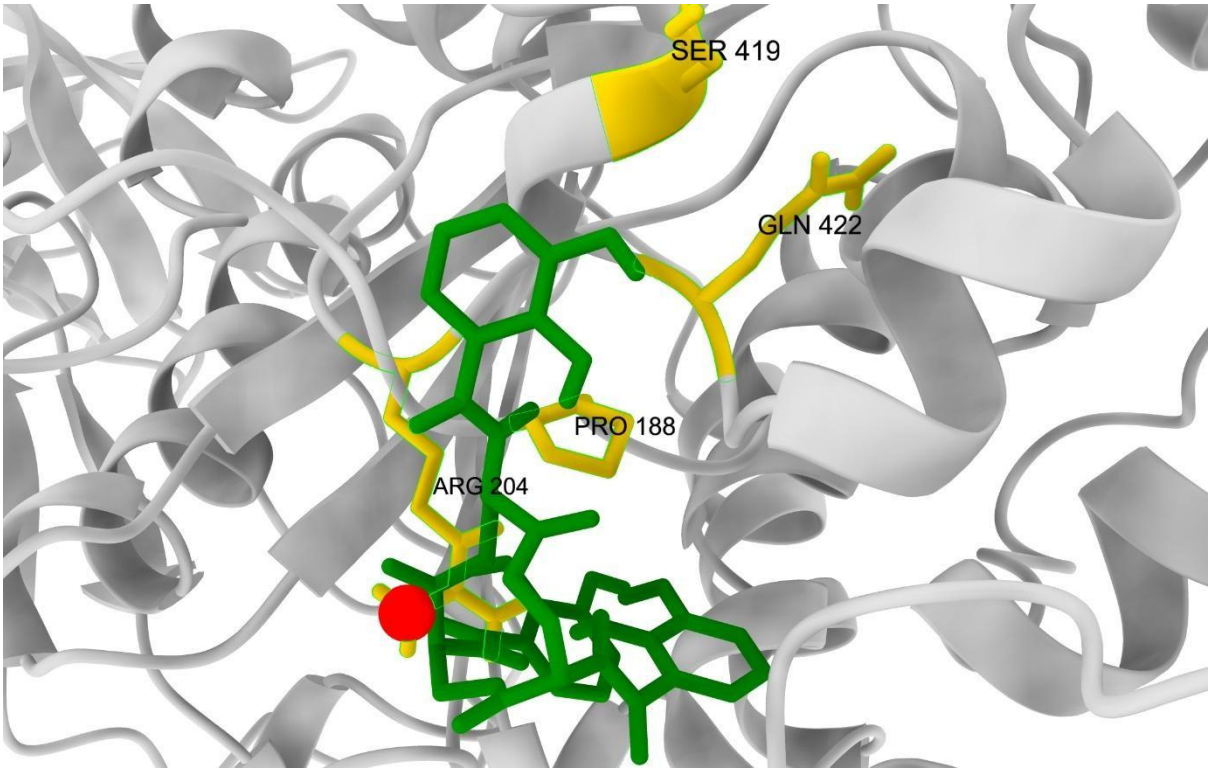
Figure S5: Approach 3.

(A) Most stable docking conformation.

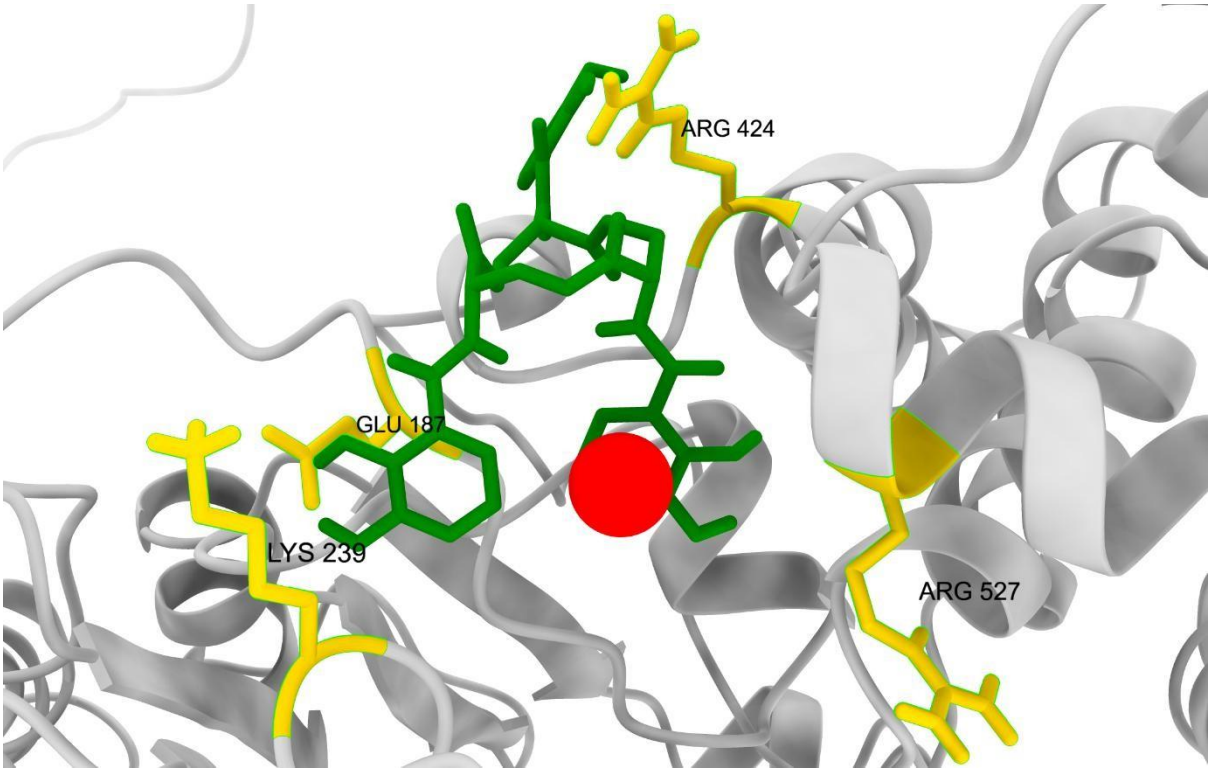
(B) Alternative conformation showing closer spatial proximity between Fe(III), enterobactin, and interacting residues. This conformation is shown for qualitative comparison and does not imply increased stability.

(C) Corresponding LIGPLOT+ interaction diagram showing interactions with Gln473, Ser220, and Tyr476.

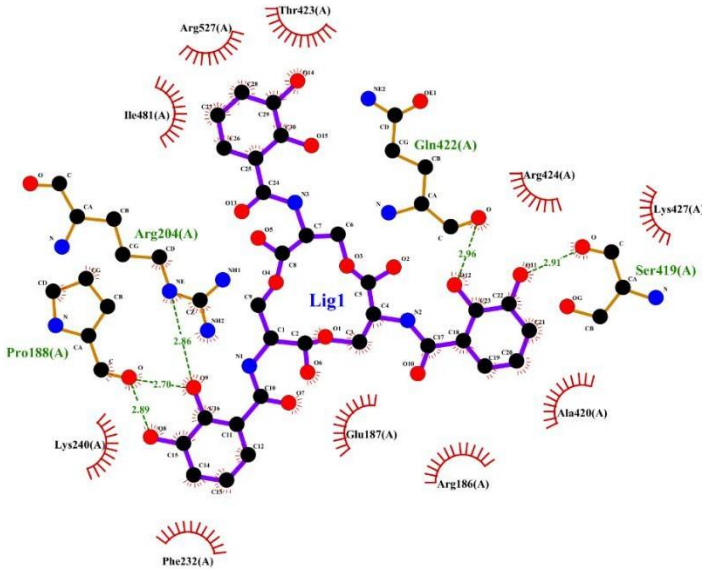
A



B



C



D

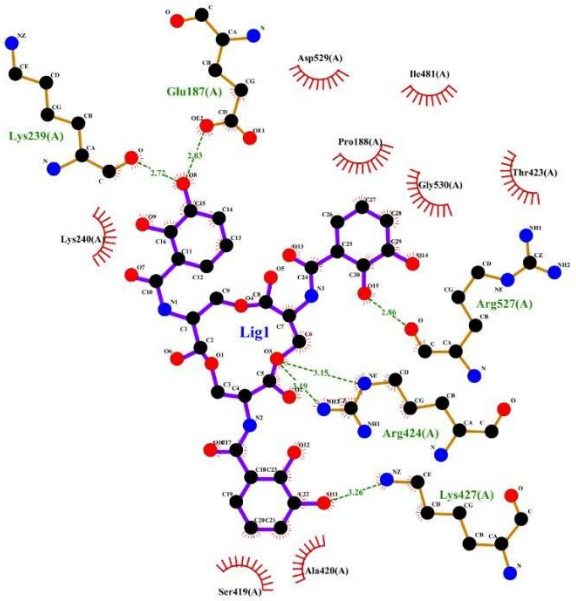


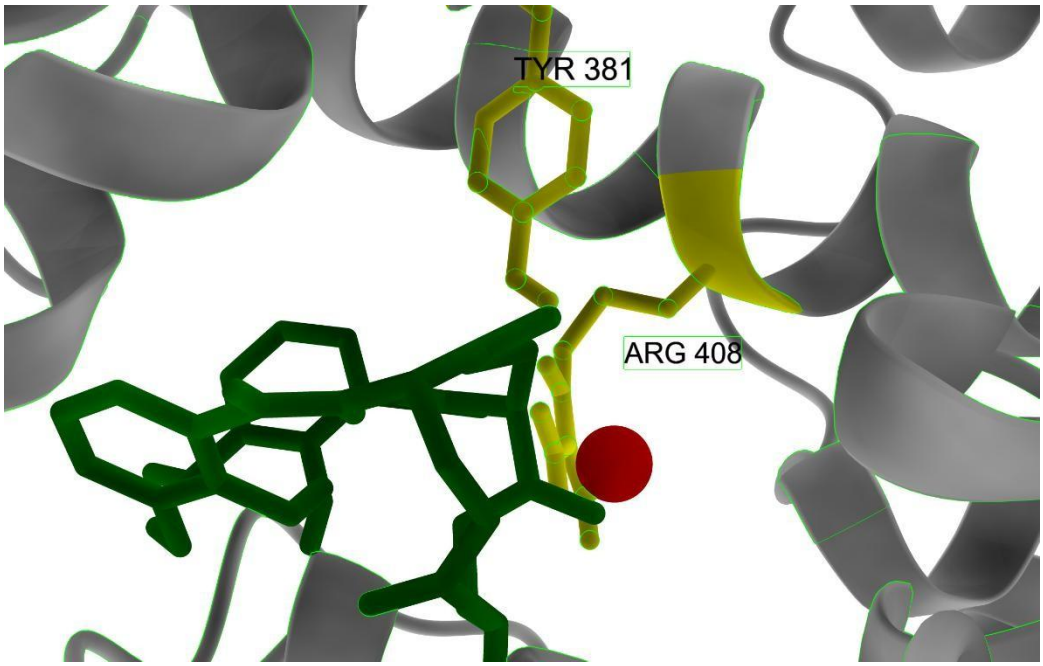
Figure S6: Approach 4.

(A) Most stable conformation obtained after docking for Approach 4a. Interacting residues include Arg204, Gln422, Ser419, and Pro188.

(B) Most stable conformation obtained after docking for Approach 4b. Interacting residues include Lys239, Gln187, Arg424, Arg527, and Lys427.

(C–D) Corresponding LIGPLOT+ interaction diagrams for Approaches 4a and 4b, respectively

A



B

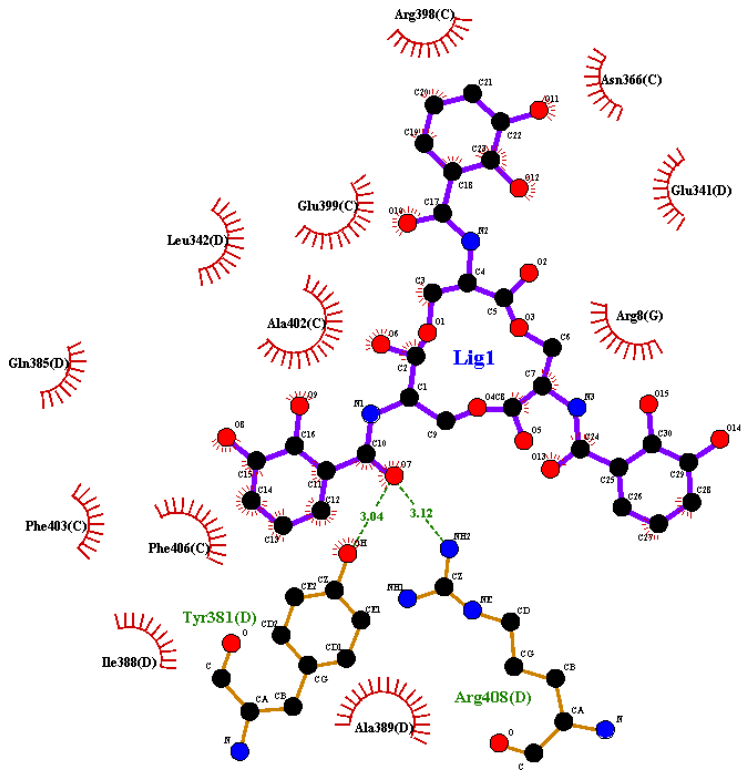


Figure S7: Bovine mitochondrial F1 ATPase docking with Fe(III)-enterobactin.

(A) Most stable docking conformation. Interacting residues (Tyr381 and Arg408) are shown in yellow.

(B) Corresponding LIGPLOT+ interaction diagram.

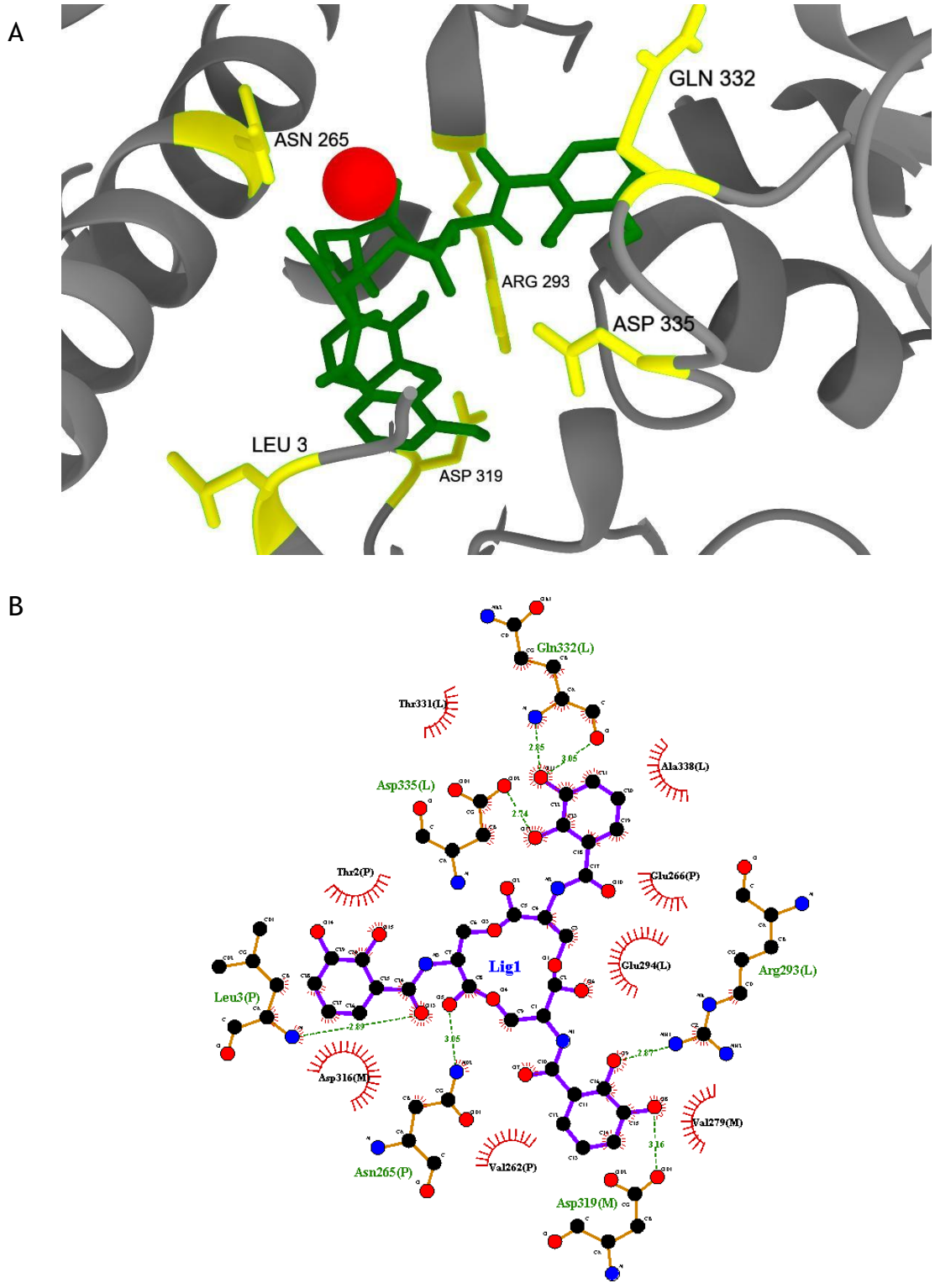


Figure S8: Yeast mitochondrial ATPase docking with Fe(III)-enterobactin.

(A) Most stable docking conformation. Interacting residues include Arg293, Gln332 and Asp335 (chain L), Leu3 and Asn265 (chain P), and Asp319 (chain M), spanning multiple subunits.

(B) Corresponding LIGPLOT+ interaction diagram.

Table S1. Comparison of Fe(III)–enterobactin coordination geometry in experimental structures and Vina-generated configurations.

Structure	**Structural basis**	**Six nearest Fe–O distances (Å)**
Ferric enterobactin	Single-crystal X-ray structure reported by Johnstone and Nolan (2017)	1.965–2.041*
PDB 6I2J	Protein-bound ferric enterobactin	2.129, 2.187, 2.198, 2.207, 2.239, 2.270
PDB 6R1F	Protein-bound ferric enterobactin	1.925, 2.029, 2.048, 2.052, 2.098, 2.175
Vina configuration 1	Fe(III)–enterobactin configuration generated in the present study	2.438, 2.605, 2.708, 3.111, 3.603, 4.572
Vina configuration 2	Fe(III)–enterobactin configuration generated in the present study	2.391, 2.398, 3.364, 3.816, 4.577, 5.157

The Fe–O range for the direct ferric-enterobactin crystal structure represents crystallographic Fe–O bond lengths reported by Johnstone and Nolan (2017). For PDB entries 6I2J and 6R1F and the two Vina-generated configurations, values represent the six shortest distances measured between Fe(III) and enterobactin oxygen atoms from the respective structural coordinate files. This comparison was used to assess the representation of Fe(III) coordination geometry and does not constitute an energetic evaluation or rescoring of the docking configurations.